Reduced bases for a three-level atom interacting with a two-mode radiation field

S. Cordero, O. Castaños, R. López-Peña,* and E. Nahmad-Achar
Instituto de Ciencias Nucleares, Universidad Nacional Autónoma de México, Apartado Postal 70-543, 04510 México Cd. Mx., Mexico

(Received 8 November 2018; published 6 March 2019)

Reduced bases are obtained for a single three-level atom interacting dipolarly with a two-mode electromagnetic field in a cavity. A truncation scheme for the infinite dimensional Hilbert space of the system is proposed, which we take it as the *exact ground-state solution*. This is used to determine the quantum phase diagram of the atomic Λ configuration and to judge the goodness of the reduced bases. This provides us with a mathematical technique that can be used to solve systems where the number of atoms and excitations grow, yielding a Hilbert space with enormous dimensions, more effectively than with the currently available methods. Additionally, the sudden changes suffered by the ground-state solution can be observed through the calculation of the purity and the occupation probabilities.

DOI: 10.1103/PhysRevA.99.033811

I. INTRODUCTION

The study of a finite number of three-level atoms interacting dipolarly with an electromagnetic field in a cavity deserves attention in applications such as quantum memories and for other quantum information and quantum optics purposes. For instance, alkali metals, as confirmed by the electromagnetically induced transparency effect, are good approximations to three-level systems in the Λ configuration, and schemes have been presented for various quantum gates using three-level atoms and trapped ions [1,2]. Moreover, off-resonant systems protect one from spontaneous emission and have thus been favored in practical applications because of their advantage when subjected to coherent manipulations. The ground-state phase diagram as a function of the coupling strengths has been established for the V-type atomic configuration and a single-mode quantized field but whose components posses different phase factors, which is very similar to our results considering two-mode radiation fields [3,4]. In many-body entanglement studies, the collective interactions between matter and light have played an important role for quantum information processing, for example, in the generation of quantum correlations and nonclassicalities, i.e., negative values of the Wigner function for the light [5,6].

Three-level atoms are only an approximation to real atoms, but the design and construction of artificial quantum structures allows one to refer to so-called artificial atoms [7–9] that possess a finite number of levels. It is therefore interesting to consider three-level systems without loss of generality. The importance of their phase diagrams has drawn the attention of some authors [10–13], and there have been various contributions to the study of their phase transitions (cf., e.g., Ref. [14] and references therein). The phase control of coherent dynamics for one three-level atom in the V configuration has been experimantally studied [15] for potential applications in quantum sensing and quantum information processing. Other studies considering one three-level atom include a reduction to an effective two-level model for the Ξ configuration [16] and the electromagnetically induced transparency beyond a steady-state analysis [17].

Recently, we have shown that a three-level system interacting dipolarly with a two-mode radiation field exhibits a universal parametric curve associated with the number of photons and the relative population between the levels, similar to what happens in a two-level system interacting with one mode of radiation field [18,19].

The purpose of this work is to establish reduced bases for a single three-level atom interacting dipolarly with a two-mode radiation field in a cavity, without using the rotating-wave approximation. This reduction is guided by the ground-state variational solution together with the parity invariants. These were used on the system as a test bed to measure their effectiveness. The quality of the reduced bases is determined by means of the calculation of the fidelity with respect to the numerically exact ground-state solution of the system. We show that the sequence of ever approximating bases for the infinite-dimensional Hilbert space leads to an excellent agreement with the exact behavior with much less expenditure. This provides us with a mathematical technique that can be used to solve systems where the numbers of atoms and excitations grow, yielding a Hilbert space with enormous dimensions, more effectively than with the currently available methods.

For the numerically exact ground-state solution, we carry out a truncation of the infinite-dimensional Hilbert space by asking for the ground state to be unchanged up to a pre-established precision. Therefore, for fixed values of the frequencies of the atomic levels and the modes of the cavity, the ground state is determined as a function of the matter-field coupling parameters. By means of the fidelity concept, the loci of points where phase transitions occur in the Λ configuration are calculated. The phase diagram exhibits continuous and discontinuous transitions. Of the four discontinuous transitions present, three are associated to changes in the parity invariants while the fourth is related to the transition between two-level subsystems, i.e., from the region S_{13} where one photon mode Ω_{13} dominates, to the region S_{23} dominated

*Corresponding author: lopez@nucleares.unam.mx

by the other mode Ω_{23}, or vice versa. For the continuous transitions, while preserving the parity, the behavior changes from a *normal* regime (where the decay is proportional to the number of atoms N_a, and there are zero photons contributing to the ground state) to a *super-radiant* regime (where the decay is proportional to N_a^2, and there is a nonzero number of photons contributing to the ground state). This behavior is clearly shown in the plots of the expectation values of the number of photons.

We make use of a sequence of ever approximating bases for the infinite-dimensional Hilbert space $\mathcal{H}$. A fidelity criterion, which may be set according to the problem to be tackled, is used to truncate the dimension of $\mathcal{H}$ and from it the one-particle phase diagram of the ground state is obtained. The parity of the ground state and the type of photons dominating the excitations is studied in each region. Guided by a ground-state variational solution, together with the help of the preserved parities of the Hamiltonian, a sequence of ever approximating reduced bases is constructed and the results obtained from these are compared with those from the exact basis. We show that a reduced basis may be chosen which leads to an excellent agreement with the exact behavior with much less expenditure. As an example, the Λ configuration is considered in detail.

This paper is organized as follows: Section II introduces the model and splits the Hilbert space into subspaces according to the preserved parities, establishing a quantitative procedure to truncate the infinite-dimensional Hilbert space of the system. The geometry of the phase diagram is also reviewed for each atomic configuration. Section III shows how to construct the sequence of reduced bases, in terms of the order parameter O given in (12). Section IV gives some applications for the Λ configuration, as, for example, the calculation of the quantum phase diagram for $N_a = 1$ by means of the fidelity concept. A comparison of the ground states associated to the reduced and exact bases is also done, and the behavior of the purity and occupation probabilities is established in the coupling parameter space. Section V presents a summary and conclusions.

II. MODEL

We consider the multipolar Hamiltonian which may be written as [4,20,21] (taking $\hbar = 1$)

$$\mathbf{H} = \mathbf{H}_D + \mathbf{H}_{\rm int}, \tag{1}$$

where $\mathbf{H}_D$ and $\mathbf{H}_{\rm int}$ are the diagonal and interaction contributions, respectively, given by

$$\mathbf{H}_D = \sum_{j<k}^{3} \Omega_{jk}\, \mathbf{a}_{jk}^{\dagger}\, \mathbf{a}_{jk} + \sum_{j=1}^{3} \omega_j\, \mathbf{A}_{jj}\,, \tag{2}$$

$$\mathbf{H}_{\rm int} = -\frac{1}{\sqrt{N_a}} \sum_{j<k}^{3} \mu_{jk} (\mathbf{A}_{jk} + \mathbf{A}_{kj})(\mathbf{a}_{jk} + \mathbf{a}_{jk}^{\dagger})\,. \tag{3}$$

Here $\mathbf{a}_{jk}^{\dagger}$, $\mathbf{a}_{jk}$ are the creation and annihilation photon operators for the mode connecting the atomic levels j and k, and $\mathbf{A}_{ij} = |i\rangle\langle j|$ are the matter operators obeying the U(3) algebra

$$[\mathbf{A}_{ij},\, \mathbf{A}_{lm}] = \delta_{jl}\, \mathbf{A}_{im} - \delta_{im}\, \mathbf{A}_{lj}\,, \tag{4}$$

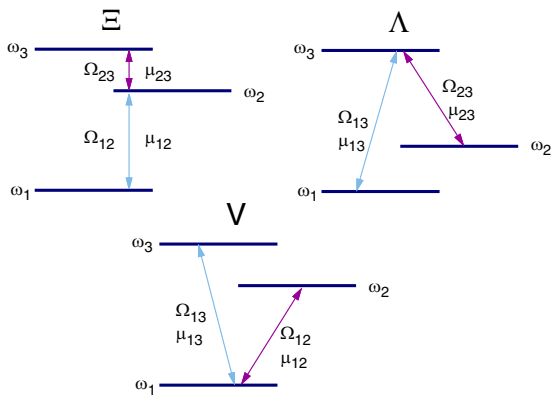

FIG. 1. Atomic configurations Ξ, Λ, and V. The ith atomic energy level ($\hbar = 1$) is denoted by ω_i with the convention $\omega_1 \leqslant \omega_2 \leqslant \omega_3$, and the coupling parameter between levels i and j is μ_{ij}. The field frequencies are denoted by Ω_{ij}.

with $\sum_{k=1}^{3} \mathbf{A}_{kk} = I$. We have denoted the field frequencies by Ω_{jk} and assumed that the atomic frequencies satisfy $\omega_1 \leqslant \omega_2 \leqslant \omega_3$. Furthermore, μ_{ij} is the coupling parameter between levels i and j, and the different atomic configurations are chosen by taking the appropriate value $\mu_{ij} = 0$ (cf. Fig. 1).

The ground-state energy for the different atomic configurations as a function of the dimensionless coupling constants $x = \mu/\mu^c$, with μ^c being the two-level critical coupling, has been calculated using the variational method and is given in Fig. 2 [4]. In addition, the separatrices (white lines, regions of points where a sudden change in the ground state of the system is happening) and their corresponding order of the quantum phase transitions are shown. In each case, we can see a normal region, N, for small values of x where atoms emit and absorb independently, and two super-radiant regions where they show a collective behavior. For large values of x, the collective subregion S_{ij} is completely dominated by photons of type ν_{ij}.

The Hamiltonian system (1) is invariant under parity transformations of the form

$$\mathbf{\Pi}_1 = e^{i\pi\,\mathbf{K}_1}\,, \quad \mathbf{\Pi}_2 = e^{i\pi\,\mathbf{K}_2}\,, \tag{5}$$

where $\mathbf{K}_s$, $s = 1, 2$, are constants of motion when the rotating-wave approximation (RWA) is taken. These are found by setting $[\mathbf{\Pi_j},\, \mathbf{H}] = 0$ and having $\mathbf{K}_s$ be a linear operator,

$$\mathbf{K}_s = \eta_{12}^{(s)}\, \boldsymbol{\nu}_{12} + \eta_{13}^{(s)}\, \boldsymbol{\nu}_{13} + \eta_{23}^{(s)}\, \boldsymbol{\nu}_{23} + \sum_{k=1}^{3} \lambda_k^{(s)}\, \mathbf{A}_{kk}\,, \tag{6}$$

where $\boldsymbol{\nu}_{12}$, $\boldsymbol{\nu}_{13}$, and $\boldsymbol{\nu}_{23}$ denote the number of photons of each one of the modes of the electromagnetic field. The coefficients of the operators are given in Table I for the different atomic configurations.

Notice that the operators $\mathbf{K}_s$ have non-negative integer eigenvalues; thus, the Hilbert space $\mathcal{H}$ can be divided into four subspaces of the form

$$\mathcal{H} = \mathcal{H}_{ee} \oplus \mathcal{H}_{eo} \oplus \mathcal{H}_{oe} \oplus \mathcal{H}_{oo}\,,$$

where the subscripts $\sigma = \{ee, eo, oe, oo\}$ denote the even e or odd o parity of Π_1 and Π_2, respectively.

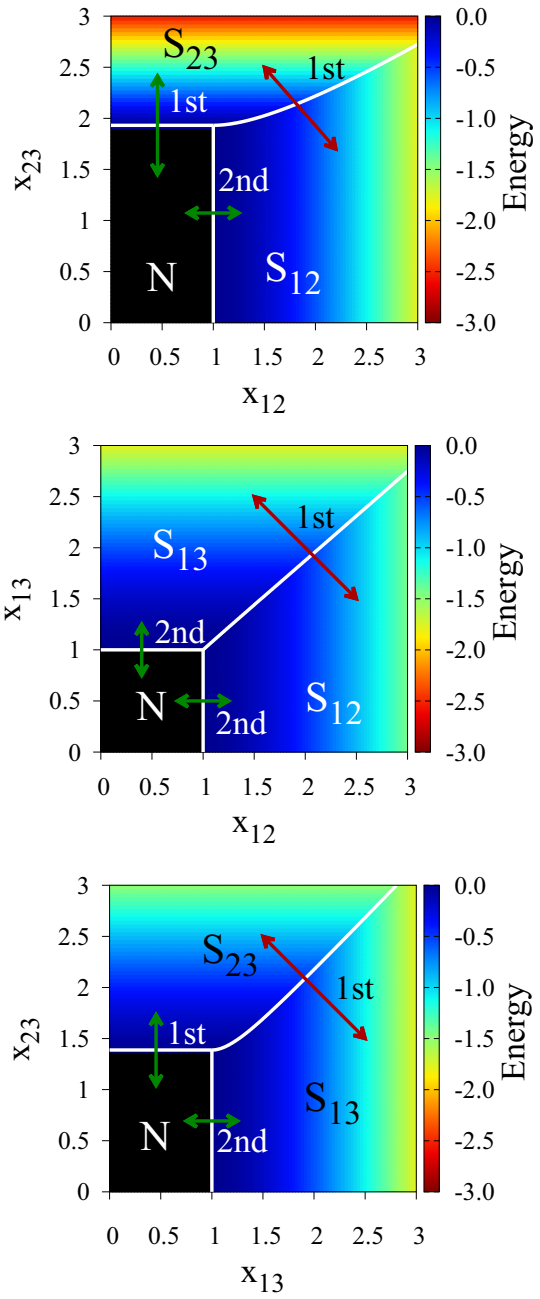

FIG. 2. Phase diagrams and energy surfaces, in resonance, for $N_a = 1$ atom in the Ξ (top), V (middle), and Λ (bottom) configurations. The separatrices (white lines) and the order of the transitions are shown. The normal regions are labeled by N (black). The superradiant region is divided into subregions S_{ij} and $S_{k\ell}$ where modes Ω_{ij} and $\Omega_{k\ell}$ dominate, respectively. In all cases, matter and field are in resonance, and the axes are $x_{ij} = \mu_{ij}/\mu_{ij}^c$, where μ_{ij}^c is the two-level critical coupling. In this and other plots, the energy is measured in units of $[\hbar\omega_3]$ and x_{ij} are dimensionless.

Given that the parity is preserved, each one of the subspaces $\mathcal{H}_\sigma$ can be written in the form

$$\mathcal{H}_\sigma = \oplus_{r=0}^{\infty}\mathcal{H}^{(\pi_1+2r,\pi_2+2r)},$$

TABLE I. Coefficients corresponding to the $\boldsymbol{K}_s$ operators in Eq. (6) are given for the atomic Λ, Ξ, and V configurations.

Conf.	$\boldsymbol{K}_s$	$\eta_{12}^{(s)}$	$\eta_{13}^{(s)}$	$\eta_{23}^{(s)}$	$\lambda_1^{(s)}$	$\lambda_2^{(s)}$	$\lambda_3^{(s)}$
Λ	$\boldsymbol{K}_1$	0	1	1	0	0	1
	$\boldsymbol{K}_2$	0	0	1	1	0	1
Ξ	$\boldsymbol{K}_1$	1	0	1	0	1	2
	$\boldsymbol{K}_2$	0	0	1	0	0	1
V	$\boldsymbol{K}_1$	1	1	0	0	1	1
	$\boldsymbol{K}_2$	0	1	0	0	0	1

with $(\pi_1, \pi_2) = \{(0,0), (0,1), (1,0), (1,1)\}$ associated to the parity of the operators $\boldsymbol{\Pi}_1$ and $\boldsymbol{\Pi}_2$, respectively, and $\mathcal{H}^{(k_1,k_2)}$ are the subspaces given by the values of $\boldsymbol{K}_1$ and $\boldsymbol{K}_2$.

Thus, a three-level atom interacting dipolarly with a two-mode field in a cavity generates an infinite-dimensional Hilbert space. The basis states are denoted by $|\nu_{12}, \nu_{13}, \nu_{23}\rangle \otimes |n_1, n_2, n_3\rangle$ with $n_1 + n_2 + n_3 = 1$ and $\nu_{jk} = 0, 1, \ldots, \infty$. A truncation criterion is therefore necessary to study the eigensystem of the Hamiltonian, and this is obtained by asking convergence of the fidelity between base states $|\,\psi(k_{1\max}, k_{2\max})\rangle$ and $|\,\psi(k_{1\max}+2, k_{2\max}+2)\rangle$, where $(k_{1\max}, k_{2\max})$ are the maximum eigenvalues taken by the operators $\mathbf{K}_1$ and $\mathbf{K}_2$ in the current approximation, to an error of the order $e_{\rm rr} = 10^{-10}$, i.e.,

$$1 - \mathcal{F}(k_1, k_2) \leqslant 10^{-10}. \tag{7}$$

where $\mathcal{F}(k_1, k_2) = |\,\langle\psi(k_1, k_2)|\psi(k_1+2, k_2+2)\rangle\,|^2$. This fidelity constraint is arbitrary and may be set according to the problem to be tackled; we have chosen the approximation given in Eq. (7) as good because we have found that to this approximation the expectation value of the energy of the ground state remains fixed up to 10^{-8} even for large values of the coupling constants. The basis $\mathcal{B}_\sigma$ so obtained will be called hereafter the *exact basis*, for the different parity Hilbert subspaces.

III. REDUCED BASES

Given the infinite-dimensional nature of the Hilbert space, and the necessity of truncating its basis to obtain what we have called the *exact* basis for operational purposes, the fact remains that this exact basis, while allowing us to calculate energies and phase transitions as will be shown below, is still the basis of a Hilbert space of large dimensions. If we want to extend this work for a larger number of atoms, the dimensions will grow unwieldy (cf. Refs. [19,22]).

This fact begs the question of whether one can still reduce the dimension of the Hilbert space while still obtaining essentially the same results as with the exact basis. The logic behind our methodology rests in two facts obtained from the variational results:

(i) We have previously derived a method [4] for reducing a system of n-level atoms interacting with radiation to a system of $(n-1)$-level atoms, where the transitions between two given atomic levels are promoted only by one mode. Applying this method iteratively, one reaches two-level systems. Thus, looking at the number of atoms to be allowed in each of

the two two-level subsystems of our three-level atom will be essential.

(ii) We have also shown [4,14] that the polychromatic phase diagram for n-level atoms interacting with ℓ modes of an electromagnetic field divides itself naturally into monochromatic subregions, where a single electromagnetic mode dominates. Then, checking the total number of excitations allowed in each of the two two-level subsystems will be crucial.

The first statement will be relevant for studies of N_a-particle systems; here we describe the methodology for constructing an ever approximating sequence of bases $\mathcal{B}_F(O)$ for $N_a = 1$ atom. For the general case of many atoms, see Ref. [22].

For three-level atoms, the phase diagram is constituted by the so-called normal region and three super-radiant subregions S_{12}, S_{13}, and S_{23}. Each one of these subregions behaves as the super-radiant region of a two-level system. Recall that only two coupling parameters are diferent from zero for each atomic configuration (cf. Fig. 1), which means that each configuration has only two super-radiant subregions.

For the particular case of two-level atoms interacting dipolarly with one mode Ω_{jk} of electromagnetic field, with $(jk) = \{(12), (13), (23)\}$, the Hamiltonian associated to the mode Ω_{jk} possesses only one parity operator, namely

$$\mathbf{\Pi}_{jk} = e^{i\pi \boldsymbol{M}_{jk}}\,, \quad \boldsymbol{M}_{jk} = \boldsymbol{\nu}_{jk} + \boldsymbol{A}_{kk}\,, \tag{8}$$

where $\boldsymbol{M}_{jk}$ stands for the total number excitations operator, which is a constant of motion when the rotating-wave approximation is considered. From the variational calculation [21], one finds that this system presents a phase transition at

$$\bar{\mu}^c_{jk} := \tfrac{1}{2}\sqrt{\Omega_{jk}\,\omega_{kj}}\,; \qquad \omega_{kj} := \omega_k - \omega_j\,,$$

where $j < k$. It is convenient to study the solutions to the three-level systems in terms of dimensionless matter-field coupling and detuning parameters,

$$x_{jk} := \frac{\mu_{jk}}{\bar{\mu}^c_{jk}}\,, \quad \Delta_{jk} := \frac{\Omega_{jk}}{\omega_{jk}} - 1\,. \tag{9}$$

In this form, all two-level systems with the same value of the detuning parameter Δ_{jk} will have the same phase diagram when plotted as a function of x_{jk}; in other words, they are equivalent.

For each one of the Hilbert spaces $\mathcal{H}_\sigma$, there is a corresponding exact basis which we denote by $\mathcal{B}_\sigma$. The matter sector constitutes a three-dimensional space generated by the Fock states, $B_M = \{|100\rangle, |010\rangle, |001\rangle\}$.

The field basis states are generated by the Fock states $\{|\nu_{12}\,\nu_{13}\,\nu_{23}\rangle\}$, where ν_{ij} denotes the eigenvalue of the photon number operator $\boldsymbol{\nu}_{ij}$. For each one of the modes $\{\Omega_{12}, \Omega_{13}, \Omega_{23}\}$, and if we ask for the ground state to be unchanged in, say, one part in 10^{-10}, a maximum number of photons can be established by the corresponding maximum eigenvalue m_{ij} of the total number of excitations operator $\mathbf{M}_{ij}$, which depends on the matter-field coupling strengths, as shown in Fig. 3. The basis states are then given by

$$B_F = \{|\nu_{12}\,\nu_{13}\,\nu_{23}\rangle \mid \nu_{ij} \leqslant m_{ij}(x_{ij})\}\,, \tag{10}$$

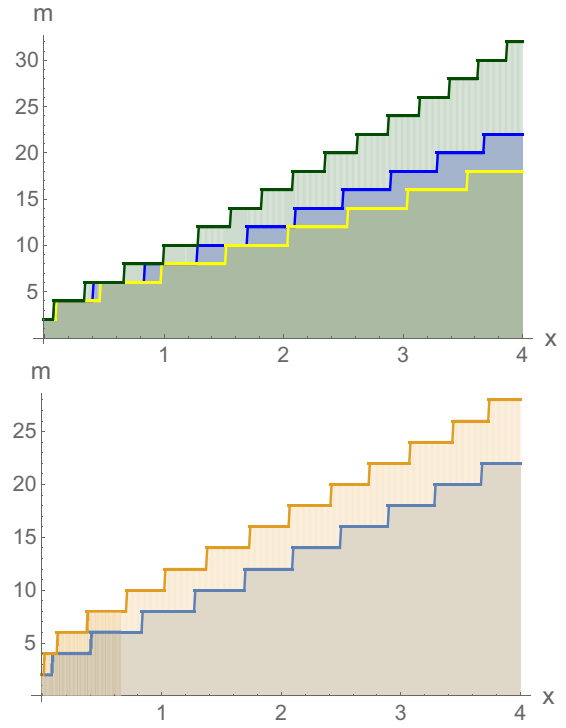

FIG. 3. Eigenvalue m of the total number of excitations operator $\mathbf{M}$ as a function of the matter-field coupling strength x. It is shown above for different detuning values: 0.5 (bottom, yellow), 0 (middle, blue), and -0.5 (top, green). Below, for resonant conditions, and for convergence to 10^{-10} (bottom, blue) and to 10^{-15} (top, orange).

with $(ij) = \{(12), (13), (23)\}$ and the exact basis for the three-level system is constructed with the tensor product $B_F \otimes B_M$.

That a truncation scheme can be proposed for the field sector of the basis states is due to the result of the variational calculation in determining the ground state of the system. In the parameter space x_{12}, x_{13}, x_{23}, there are subregions where only one mode of the electromagnetic field dominates.

For instance, if we are in the S_{12} sector, we take $\nu_{12} \leqslant m_{12}(x_{12})$ and for the other electromagnetic modes we propose the truncation,

$$\begin{aligned} B_{F_{12}}(O) = \{&|\nu_{12}\,\nu_{13}\,\nu_{23}\rangle \mid \nu_{12} \leqslant m_{12}(x_{12})\,,\\ &\nu_{13} \leqslant \min\{2\,O+1\,, m_{13}(x_{13})\}\,,\\ &\nu_{23} \leqslant \min\{2\,O+1\,, m_{23}(x_{23})\}\}, \end{aligned} \tag{11}$$

with the order O in the interval

$$0 \leqslant O \leqslant \max\left\{\left\lfloor \frac{m_{12}(x_{12})}{2}\right\rfloor, \left\lfloor \frac{m_{13}(x_{13})}{2}\right\rfloor, \left\lfloor \frac{m_{23}(x_{23})}{2}\right\rfloor\right\}. \tag{12}$$

Similar expressions can be obtained for the other subregions of the collective behavior of the three-level system.

Then the ordered sequence of reduced bases for the electromagnetic field can be written as the direct sum of the basis states for the different subregions,

$$B_F(O) := B_{F_{12}}(O) \oplus B_{F_{13}}(O) \oplus B_{F_{23}}(O)\,. \tag{13}$$

TABLE II. Maximum values $\tilde{r}_j$ as function of the $\tilde{k}_j$ for each parity.

σ	(π_1, π_2)	$\pi_1 + 2\,\tilde{r}_1$	$\pi_2 + 2\,\tilde{r}_2$
(e, e)	(0,0)	$\tilde{k}_1$	$\tilde{k}_2$
(e, o)	(0,1)	$\tilde{k}_1$	$\tilde{k}_2 + 1$
(o, e)	(1,0)	$\tilde{k}_1 + 1$	$\tilde{k}_2$
(o, o)	(1,1)	$\tilde{k}_1 + 1$	$\tilde{k}_2 + 1$

Therefore the reduced bases are obtained by the tensorial product $\mathcal{B}_\sigma(O) = B_F(O) \otimes B_M$, with O indicating the approximation order.

IV. APPLICATION TO THE Λ CONFIGURATION

As an example, we consider the atomic Λ configuration in the resonant case, $\Delta_{13} = \Delta_{23} = 0$ [cf. Eq. (9)], with atomic levels $\omega_1 = 0$, $\omega_2 = 1/10$, and $\omega_3 = 1$, where all the energies are normalized in units of ω_3.

The operators $\mathbf{K}_1$ and $\mathbf{K}_2$ in Eq. (5) may be selected as (cf. Table I)

$$\begin{aligned} \mathbf{K}_1 &= \boldsymbol{\nu}_{13} + \boldsymbol{\nu}_{23} + \mathbf{A}_{33} = \mathbf{M}_{13} + \boldsymbol{\nu}_{23}\,, \\ \mathbf{K}_2 &= \boldsymbol{\nu}_{23} + \mathbf{A}_{11} + \mathbf{A}_{33} = \mathbf{M}_{23} + \mathbf{A}_{11}\,, \end{aligned} \tag{14}$$

where $\mathbf{M}_{13}$ and $\mathbf{M}_{23}$ denote the total number of excitations of the two-level subsystems.

Following the procedure indicated in the previous section, we ask convergence of the fidelity between base states $|\,\psi(k_{1\max}, k_{2\max})\rangle$ and $|\,\psi(k_{1\max}+2, k_{2\max}+2)\rangle$, where $(k_{1\max}, k_{2\max})$ are the maximum values for the operators $\mathbf{K}_1$ and $\mathbf{K}_2$, to an error of the order $\mathrm{e_{rr}} = 10^{-10}$ [cf. Eq. (7)]. Hereafter, we define $\tilde{k}_1 = k_{1\max}$ and $\tilde{k}_2 = k_{2\max}$. These maxima are determined as follows:

Consider *any* arbitrary two-level subsystem. Since x in Eq. (9) is a normalized coupling strength, the minimum eigenvalue m of $\mathbf{M}$ in Eq. (14) which satisfies the criterion in Eq. (7) will be the maximum value m needed for the construction of the basis. This leads to

$$\tilde{k}_1 = m_{13}(x_{13}) + m_{23}(x_{23})\,, \quad \tilde{k}_2 = m_{23}(x_{23}) + 1\,. \tag{15}$$

By assuming that the maximum values of the last expressions are even integers, one is able to establish the basis states for the four parity subspaces mentioned before, as shown in Table II. (If one of them is not even, we add 1 to it without losing precision.)

We have proved that the values given in Eq. (15) satisfy the fidelity criterion. The exact basis so constructed will be denoted by $\mathcal{B}_\sigma$.

The ground state of the system, for any parity Hilbert space σ [denoted also by (π_1, π_2)], may be written as

$$\begin{aligned} &|\Psi(x_{13}, x_{23})\rangle_{\pi_1,\pi_2} \\ &= \sum_{r_1=0}^{\tilde{r}_1} \sum_{r_2=0}^{\tilde{r}_2} \sum_{n_2,n_3=0}^{1} c_{n_2,n_3}(\pi_1 + 2\,r_1, \pi_2 + 2\,r_2) \\ &\quad \times |\pi_1 + 2\,r_1 - \pi_2 - 2\,r_2 - n_2 - n_3 - 1, \pi_2 \\ &\quad + 2\,r_2 + n_2 - 1\rangle \otimes |1 - n_2 - n_3, n_2, n_3\rangle\,, \end{aligned} \tag{16}$$

where the Fock states for the field and matter sectors appear in the second row. The π_j and $\tilde{r}_j$ values can be taken from Table II. The coefficients c_{n_2,n_3} are obtained by diagonalizing the Hamiltonian matrix for given values of x_{13} and x_{23}, with respect to the exact basis.

In this way, for each parity subspace of the Hilbert space, one is able to determine the lowest energy state of the atomic configuration as a function of the dimensionless coupling constants x_{13}, and x_{23}. From these four lowest energy states, we select the global minimum of the energy, called the quantum energy surface E_Λ of the system

$$E_\Lambda = \min\{E_{ee}, E_{eo}, E_{oe}, E_{oo}\}\,, \tag{17}$$

together with the corresponding eigenstates.

This quantum minimum energy surface may be compared with the variational energy surface given in Fig. 2. By means of a similar procedure, the quantum energy surfaces of the Ξ and V atomic configurations can be obtained.

A. Phase diagram

The fidelity concept emerges in classical information theory, which measures the accuracy of a transmission in a communication protocol [23]. In the 1990s, it was introduced in the quantum information formalism as a measure of the similarity between two probability distributions or as the overlap of the input qubit with the output in a transmission of information process. This can be, for example, the overlap between the input qubit and the teleported one.

A tool based on the fidelity and fidelity susceptibility to determine the quantum phase transitions of a physical system has been proposed [21,24,25]. Here, we use it to calculate the overlap of the ground state of the system, for certain values of the coupling strengths, with the corresponding ground state with an infinitesimal change in the parameters x_{13} or x_{23}, i.e.,

$$\mathcal{F} = |\langle\Psi(x_{13} + \delta x_{13}, x_{23} + \delta x_{33})|\Psi(x_{13}, x_{23})\rangle|^2\,. \tag{18}$$

When the fidelity reaches its minimum value, one can say that there is a singularity in the system which leads to a phase transition in its ground state. The actual procedure is carried out by fixing the dipolar strength x_{13} and leaving x_{23} free or vice versa, for all the selected range in parameter space. Notice that one may also calculate the overlap of the ground state of the system with an arbitrary representative state of the Hilbert space in order to detect the sudden changes in the structure of the ground state of the system [26].

Figure 4 (top) shows, for the ground state of the Λ configuration, the quantum phase diagram so obtained superimposed on the energy surface. The structure of the ground state changes significantly in each region. Each transition across the darker (black) lines changes the parity of the subspace where the ground state lies. At top left, the ground state lies in $\mathcal{H}_{ee}$, at bottom right it is in $\mathcal{H}_{eo}$, and in the middle region it lies in $\mathcal{H}_{oo}$. Figure 4 (bottom) shows the contour plot of the fidelity. Once again, the darker (black) lines show changes in the parity of the ground state. The blue lines (thicker, at bottom right and upper left) and orange lines (thicker, at upper right) show continuous phase transitions where the parity is conserved. The transitions crossing the blue lines keep the same kind of

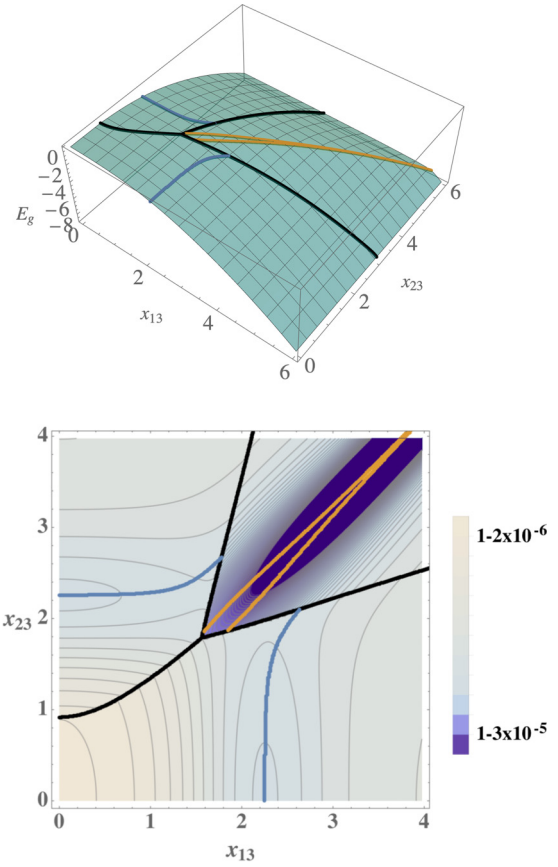

FIG. 4. For the atomic Λ configuration in parameter space $\{x_{13}, x_{23}\}$, we show the quantum phase diagram on the energy surface (top) and the contour plot of the fidelity (bottom), for the ground state, showing the regions where the ground state changes significantly. The darker (black) lines show changes in the parity of the ground state. The blue lines (thicker, at bottom right and upper left) and orange lines (thicker, at upper right) show continuous phase transitions where the parity is conserved. The transitions crossing the blue lines keep the same kind of photons, while across the orange lines the kind of photon that dominates changes.

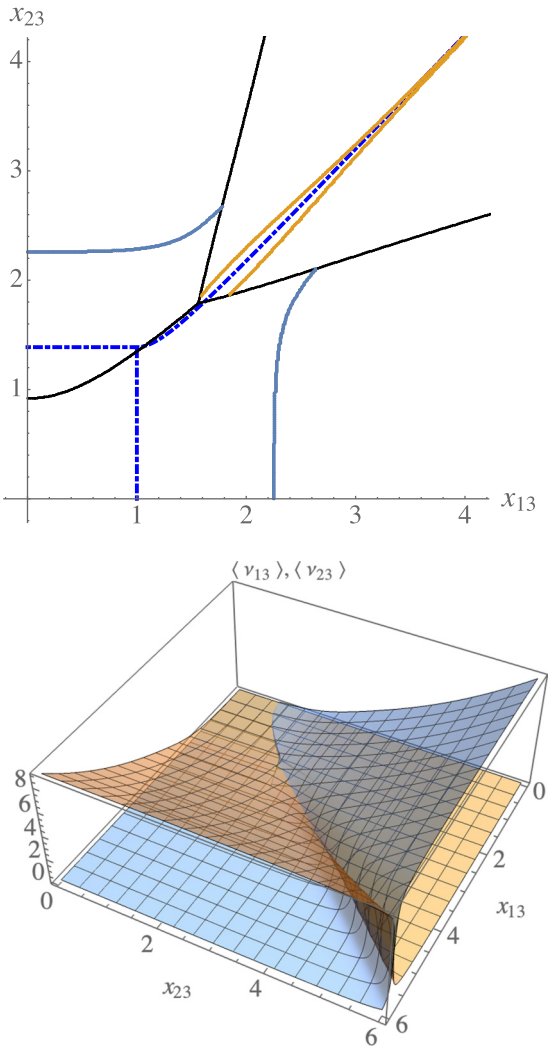

FIG. 5. Top: Comparison of the quantum phase diagrams for $N_a = 1$ (solid lines) and $N_a \to \infty$ (dot-dashed blue curve). Bottom: Expectation value of the number of photons for each mode, in the Λ configuration.

photons, while across the orange lines the kind of photon that dominates changes.

A quantum phase diagram for a finite number of atoms for the V configuration in the corresponding parameter space has been found by means of a similar procedure. In this case, the even-even parity subspace dominates completely and in consequence there are no parity transitions in the ground state [19].

Figure 5 (top) compares the quantum phase diagrams for $N_a = 1$ (solid lines) and $N_a \to \infty$ (dot-dashed blue curve). This latter phase diagram is independent of the parity, so the surface energy for it completely lies in $\mathcal{H}_{ee}$. Preliminary calculations show that, as N_a increases, the thick black lines where the parity of the ground state changes closes in toward the thermodynamic phase transition, and the thick blue lines where the transition keeps the photon kind slide towards the vertical and horizontal thermodynamic transitions. The same is suggested from calculations for three-level systems with one radiation mode [12]. Figure 5 (bottom) shows the expectation value of the number of photons for each mode. We see that even when we have a single atom, the loci where the number of photons for each mode grows significantly different from zero follows exactly the phase transition of the variational solution for $N_a \to \infty$.

This plot also shows a continuous quantum phase transition within the collective regime, from a region in which one mode dominates to another where the roles of the photon types are interchanged.

B. Exact vs reduced basis states

Following the procedure described above for generating reduced bases, Table III shows the dimension of each Hilbert subspace for different reduction orders $\mathcal{B}_{\pi_1,\pi_2}(O)$. For the two-level system in resonance, at $x = 4$, we have $m = 22$, so the exact basis, from Eq. (12), is $\mathcal{B}_{\pi_1,\pi_2} = \mathcal{B}_{\pi_1,\pi_2}(11)$. Note that there is a difference of a factor greater than 2 between the dimension of the full Hilbert subspace and the one reduced to order 0.

TABLE III. Dimension of the Hilbert subspaces for different reduction orders $\mathcal{B}_{\pi_1,\pi_2}(O)$.

O	$\mathcal{B}_{0,0}(O)$	$\mathcal{B}_{0,1}(O)$	$\mathcal{B}_{1,0}(O)$	$\mathcal{B}_{1,1}(O)$
0	177	165	166	176
1	218	205	207	216
2	255	241	244	252
3	288	273	277	284
4	317	301	306	312
5	342	325	331	336
6	363	345	352	356
7	380	361	369	372
8	393	373	382	384
9	402	381	391	392
10	407	385	396	396
11	408	385	396	396

The ground-state energy surface is determined together with the corresponding eigenvectors in the coupling parameter space.

The exact basis $\mathcal{B}$ for the ground state is taken from the lowest energy state of each one of the parity sectors, that is, from the energy surface [cf. Eq. (17)]. As shown in Fig. 4, the ground state is constituted by one of the Hilbert subspaces $\mathcal{H}_{ee}$, $\mathcal{H}_{eo}$, and $\mathcal{H}_{oo}$, depending on the coupling values x_{13} and x_{23}. We proceed similarly for the reduced basis $\mathcal{B}(O)$.

The fidelity between the ground state of the exact basis $\mathcal{B}$ and the ground state obtained by using the reduced basis $\mathcal{B}(0)$, $\mathcal{B}(1)$, and $\mathcal{B}(2)$ is shown in Fig. 6. Note the scale of the ordinate axes: For the $\mathcal{B}(2)$ basis the disagreement between the ground states is of the order of 10^{-8} at most, and only in a vicinity of the phase transition between the collective regions. Even for the $\mathcal{B}(1)$ basis, the disagreement is of the order of 10^{-5} at most. This means that, depending on the properties under study and their purpose, using our reduced bases leads to excellent agreement with the exact behavior with much less expenditure.

C. Purity and occupation probabilities

The object under study is a pure bipartite matter-field system, for which the entanglement may be calculated by means of the linear entropy or the von Neumann entropy. For our purposes, the linear entropy is enough, and this is defined as $1 - P$ where P is the purity of the reduced density matrix for the matter or for the field sectors. We use here the matter reduced density matrix

$$\boldsymbol{\rho}_M = \mathrm{tr}_F(|\psi_{gs}\rangle\langle\psi_{gs}|)\,. \tag{19}$$

The purity of (the matter sector of) the quantum ground state is defined as $\mathrm{tr}(\rho_M^2)$, and measures the quantum correlations between matter and field. This is shown along circumferences of different radii, drawn over the quantum phase diagram for both the $N_a = 1$ and $N_a \to \infty$ cases, in Fig. 7 for the exact basis $\mathcal{B}$. A pure state in the normal region becomes more entangled as we move out into the super-radiant regions. In the vicinity of the separatrix, the purity falls even further.

To obtain the occupation probability for each atomic level ω_i, we use Eq. (19) to calculate

$$\langle \mathbf{A}_{ii} \rangle = \mathrm{tr}(\boldsymbol{\rho}_M \mathbf{A}_{ii})\,. \tag{20}$$

For the exact basis $\mathcal{B}$, the occupation probability for the Λ configuration, along circumferences of different radii, is shown in Fig. 8. The red dots correspond to the population of level 1 and the green dots to the population of level 2. These are drawn over the quantum phase diagram for both the $N_a = 1$ and $N_a \to \infty$ cases. Note the change of roles of the occupation probabilities for the levels as one crosses the main separatrix, indicating that the behavior of the quantum ground state is governed by a two-level subsystem. It is important to also note that the occupation probability detects the phase transition.

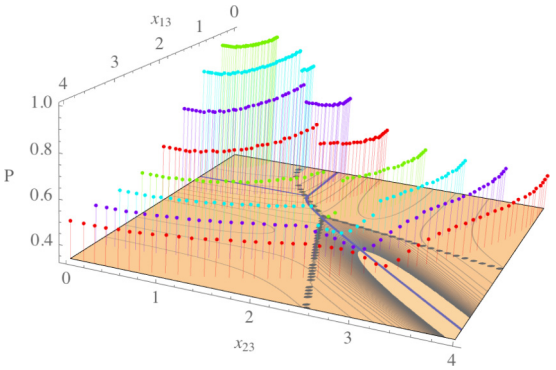

FIG. 7. Purity of the ground state along circumferences of different radii, drawn over the quantum phase diagram for both the $N_a = 1$ and $N_a \to \infty$ cases. $N_a \to \infty$ corresponds to the continuous, blue lines; same as the white lines shown in Fig. 2 bottom.

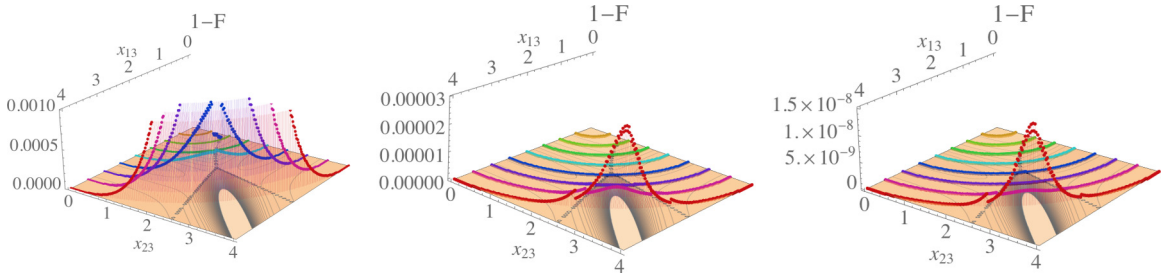

FIG. 6. Fidelity between the ground state of the exact basis $\mathcal{B}$ and the ground state obtained by using the $\mathcal{B}(0)$ basis (left), the $\mathcal{B}(1)$ basis (middle), and the $\mathcal{B}(2)$ basis (right).

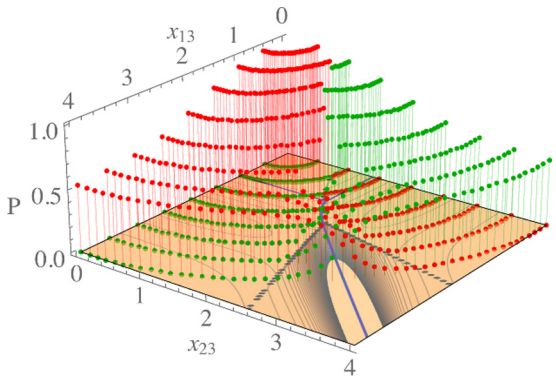

FIG. 8. Occupation probability for the Λ configuration, along circumferences of different radii. The red dots correspond to the population of level 1 and the green dots to the population of level 2. These are drawn over the quantum phase diagram for both the $N_a = 1$ and $N_a \to \infty$ cases. $N_a \to \infty$ corresponds to the continuous, blue lines, the same as the white lines shown in Fig. 2 bottom.

V. SUMMARY AND CONCLUSIONS

The quantum phase diagram for a single three-level atom interacting with a two-mode electromagnetic field was determined in the generalized Dicke model. It comprises three regions with well-defined parity. The behavior of the ground state is dominated by a two-level subsystem in two of these regions. In the third region, the quantum ground state is governed by an excited state of the two-level subsystem.

By using a fidelity criterion, an efficient way to truncate the infinite-dimensional Hilbert space for a three-level atom interacting dipolarly with a two-mode radiation field in a cavity was presented. The criterion used here was $1 - \mathcal{F} \leqslant 10^{-10}$. This fidelity constraint is arbitrary and may be set according to the problem to be tackled; we have chosen the approximation given in Eq. (7) as good because we have found that to this approximation the expectation value of the energy of the ground state remains fixed up to 10^{-8} even for large values of the coupling constants.

The exact truncated basis allowed us to obtain the finite phase diagram of the ground state and compare it with the phase diagram for the limit $N_a \to \infty$. For $N_a = 1$, we see the radical changes of the ground state as we cross from one region to another, not only in shape but in parity and in the type of photons that the state has. In fact, the expectation value in the number of photons for each mode grows significantly different from zero precisely at the separatrix for $N_a \to \infty$.

A sequence of ever approximating reduced bases was constructed guided by the ground-state variational solution together with the help of the constants of motion of the system. The fidelity was once again used to compare the properties obtained from these reduced bases with those from the exact solution. We have shown that we can get a disagreement of the order of 10^{-8} at most, and only in a vicinity of the phase transition between the collective regions, by using a basis with half the number of states. With an even smaller basis, the disagreement is of the order of 10^{-5} at most. This means that, depending on the properties under study and their purpose, using our reduced bases leads to excellent agreement with the exact behavior with much less expenditure, and this mathematical method allows for the study of systems with a large number of atoms and/or excitations [22].

The quantum correlations between matter and field have been calculated using the purity of the matter sector of the ground state. We observe that a pure state in the normal region becomes more entangled as we move out into the super-radiant subregions. In the vicinity of the separatrix, the purity falls even further.

Finally, by using the reduced density matrix for the matter sector, the occupation probability was calculated and we see that it is very sensitive to the phase transitions, as expected.

This work may be extended to multilevel atoms, larger number of atoms, and indeed many-body systems (work in progress).

ACKNOWLEDGMENTS

This work was partially supported by CONACyT-México (under Project No. 238494), and DGAPA-UNAM (under Project No. IN101217).

[1] X. X. Yi, X. H. Su, and L. You, Phys. Rev. Lett. **90**, 097902 (2003).
[2] E. Jané, M. B. Plenio, and D. Jonathan, Phys. Rev. A **65**, 050302 (2002).
[3] J. Fan, L. Yu, G. Chen, and S. Jia, Sci. Rep. **6**, 25192 (2016).
[4] S. Cordero, E. Nahmad-Achar, R. López-Peña, and O. Castaños, Phys. Rev. A **92**, 053843 (2015).
[5] O. Castaños, S. Cordero, R. López-Peña, and E. Nahmad-Achar, Phys. Scr. **93**, 085102 (2018).
[6] F. J. Gómez-Ruiz, O. L. Acevedo, F. J. Rodríguez, L. Quiroga, and N. F. Johnson, Front. Phys. **6**, 92 (2018).
[7] M. A. Kastner, Phys. Today **46**, 24 (1993).
[8] O. Astafiev, A. M. Zagoskin, A. A. Abdumalikov Jr., Yu. A. Pashkin, T. Yamamoto, K. Inomata, Y. Nakamura, and J. S. Tsai, Science **327**, 840 (2010).
[9] I. Buluta, S. Ashhab, and F. Nori, Rep. Prog. Phys. **74**, 104401 (2011).
[10] M. Hayn, C. Emary, and T. Brandes, Phys. Rev. A **84**, 053856 (2011).
[11] M. Hayn, C. Emary, and T. Brandes, Phys. Rev. A **86**, 063822 (2012).
[12] S. Cordero, R. López-Peña, O. Castaños, and E. Nahmad-Achar, Phys. Rev. A **87**, 023805 (2013).
[13] A. Baksic, P. Nataf, and C. Ciuti, Phys. Rev. A **87**, 023813 (2013).
[14] S. Cordero, E. Nahmad-Achar, O. Castaños, and R. López-Peña, Phys. Scr. **92**, 044004 (2017).
[15] A. Barfuss, J. Kölbl, L. Thiel, J. Teissier, M. Kasperczyk, and P. Maletinsky, Nat. Phys. **14**, 1087 (2018).
[16] Y. Wu and X. Yang, Phys. Rev. A **56**, 2443 (1997).
[17] Y. Wu and X. Yang, Phys. Rev. A **71**, 053806 (2005).

[18] O. Castaños, E. Nahmad-Achar, R. López-Peña, and J. G. Hirsch, Phys. Rev. A **84**, 013819 (2011).
[19] O. Castaños, S. Cordero, E. Nahmad-Achar, and R. López-Peña, J. Phys.: Conf. Ser. **1071**, 012006 (2018).
[20] O. Castaños, S. Cordero, R. López-Peña, and E. Nahmad-Achar, *Latin America Optics and Photonics Conference (LAOP)*, OSA Tech. Digest (Optical Society of America, 2014), paper LTu2B.3.
[21] E. Nahmad-Achar, S. Cordero, O. Castaños, and R. López-Peña, Phys. Scr. **90**, 074026 (2015).
[22] S. Cordero, O. Castaños, R. López-Peña, and E. Nahmad-Achar (unpublished).
[23] G. Benenti, G. Casati, and G. Strini, *Principles of Quantum Computation and Information* (World Scientific, Singapore, 2007).
[24] P. Zanardi and N. Paunkovic, Phys. Rev. E **74**, 031123 (2006).
[25] S.-J. Gu, Int. J. Mod. Phys. B **24**, 4371 (2010).
[26] O. Castaños, R. López-Peña, E. Nahmad-Achar, and J. G. Hirsch, J. Phys.: Conf. Ser. **387**, 012021 (2012).